Electronic Supporting Information

# Ionic liquid induced highly dense assembly of porphyrin in MOF nanosheets for photodynamic therapy

Jian-Hua Qin,[a] Hua Zhang,[b] Pengfei Sun,*[b] Ya-Dan Huang,[a] Qingming Shen,*[b] Xiao-Gang Yang,[a] and Lu-Fang Ma*[a]

[a]College of Chemistry and Chemical Engineering, Henan Key Laboratory of Function-Oriented Porous Materials, Luoyang Normal University, Luoyang 471934, China. E-mail: mazhuxp@126.com

[b]Key Laboratory for Organic Electronics and Information Displays & Jiangsu Key Laboratory for Biosensors, Institute of Advanced Materials (IAM), Jiangsu National Synergetic Innovation Center for Advanced Materials (SICAM), Nanjing University of Posts & Telecommunications, 9 Wenyuan Road, Nanjing 210023, China. E-mail: iampfsun@njupt.edu.cn, iamqmshen@njupt.edu.cn

## A. Experimental Section



## B. Supporting Figures



## C. Supporting Tables



## D. Supporting References

## A. Experimental Section

### 1. Materials and general procedures.

MCF-7 breast cancer cells were obtained from the Shanghai Laboratory Animal Center, Chinese Academy of Science (SLACCAS). The Annexin V-FITC/propidium iodide (PI) cell apoptosis kit was obtained from KeyGen Biotech. Co., Ltd (Nanjing, China). Dulbecco's Modified Eagle's Medium (DMEM, Gibco, U.S.) was obtained from Gene Tech Co. (Shanghai, China). Other reagents were of analytical grade and obtained from commercial sources without further purification.

Powder X-ray diffraction analyses (PXRD) patterns were collected on a Bruker D8-ADVANCE X-ray diffractometer with Cu *Kα* radiation (λ = 1.5418 Å). Measurements were made in a 2θ range of 5−50° at room temperature with a step of 0.02° (2*θ*) and a counting time of 0.2 s/ step. The operating power was 40 KV, 30 mA. Thermogravimetric analysis (TGA) experiments were carried out using SII EXStar6000 TG/DTA6300 thermal analyzer from room temperature to 800 $^{o}$C under a nitrogen atmosphere at a heating rate of 10 $^{o}$C min$^{-1}$. UV-vis absorption spectra was measured using a Shimadzu UV-3600 plus UV-vis-NIR spectrophotometer. Room temperature PL spectra were recorded on a Hitachi 850 fluorescence spectrophotometer. Transmission electron microscope (TEM), high-resolution TEM (HR-TEM), and energy-dispersive X-ray spectroscopy (EDS) analysis were carried out on a FEI Tecnai G2 F20 instrument. The 3-(4,5-Dimethylthiazol-2-yl)-2,5-diphenyltetrazolium bromide (MTT) assay was conducted using a PowerWave XS/XS2 microplate spectrophotometer (BioTek, Winooski, VT). The flow cytometry experiments were performed using a Flow Sight Imaging Flow Cytometer (Merck Millipore, Darmstadt, Germany).

### 2. X-ray crystallography.

Single crystal X-ray diffraction analysis of **1** was carried out on an Oxford Diffraction Super Nova area-detector diffractometer using mirror optics monochromated Mo Kα radiation (λ = 0.71073 Å) at room temperature. Using Olex2[1], the structure was solved with the ShelXT[2] structure solution program using Intrinsic Phasing and refined with the ShelXL[3] refinement package using Least Squares minimisation. The hydrogen atoms were assigned with common isotropic displacement factors and included in the final refinement by use of geometrical restrains. The $[BMI]^{+}$ cations were disordered and could not be located. The diffuse electron densities in the structure were therefore treated using the SQUEEZE routine in the program PLATON. The crystallographic data and selected bond lengths and angles for **1** are listed in Tables S1-S3. Crystallographic data for the structural analyses have been deposited with the Cambridge Crystallographic Data Center. CCDC numbers for **1** is 2008501. This material can be obtained

free of charge via http://www.ccdc.cam.ac.uk/conts/retrieving.html, or from the Cambridge Crystallographic Data Centre, 12 Union Road, Cambridge CB2 1EZ, UK; fax: (+44) 1223-336-033; or E-mail: deposit@ccdc.cam.ac.uk.

## B. Supporting Figures

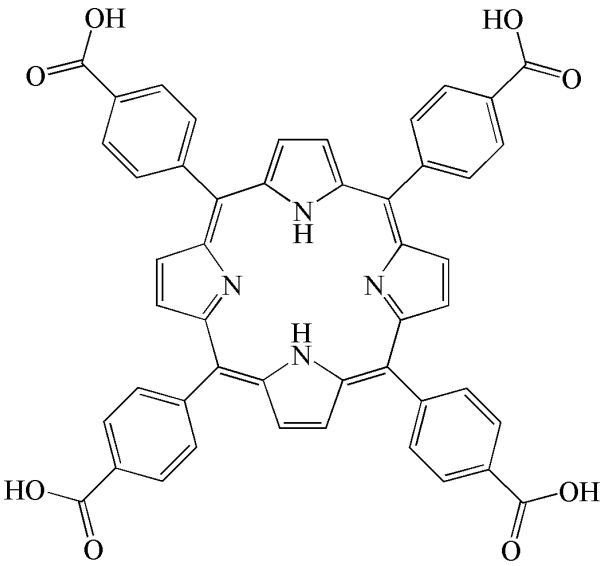

(a)

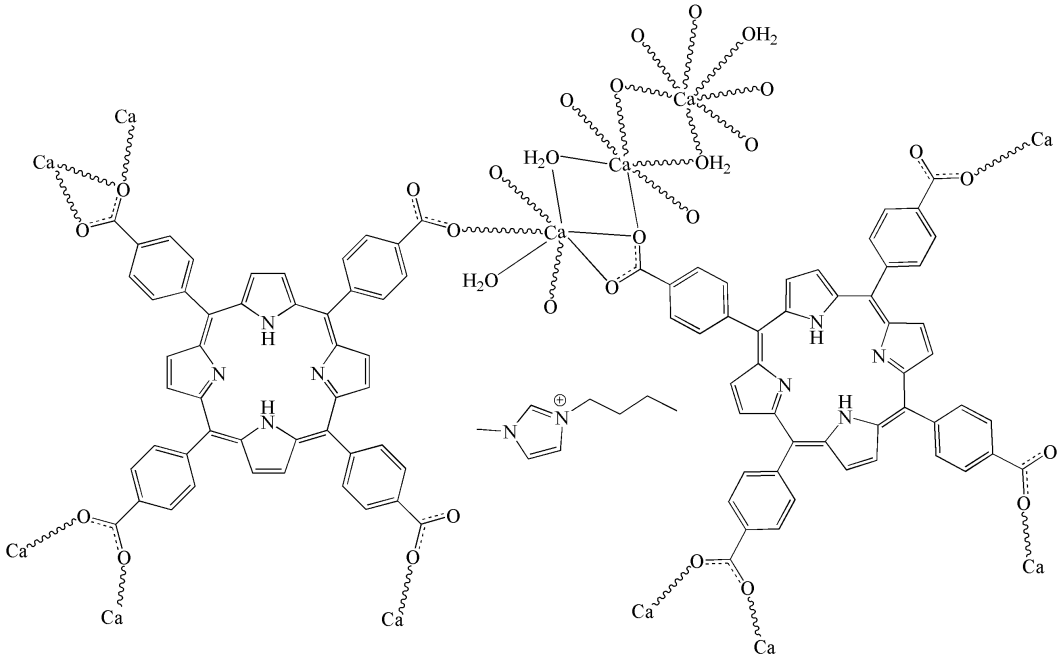

(b)

**Fig. S1** The molecular structure of $H_6TCPP$ (a) and **1** (a).

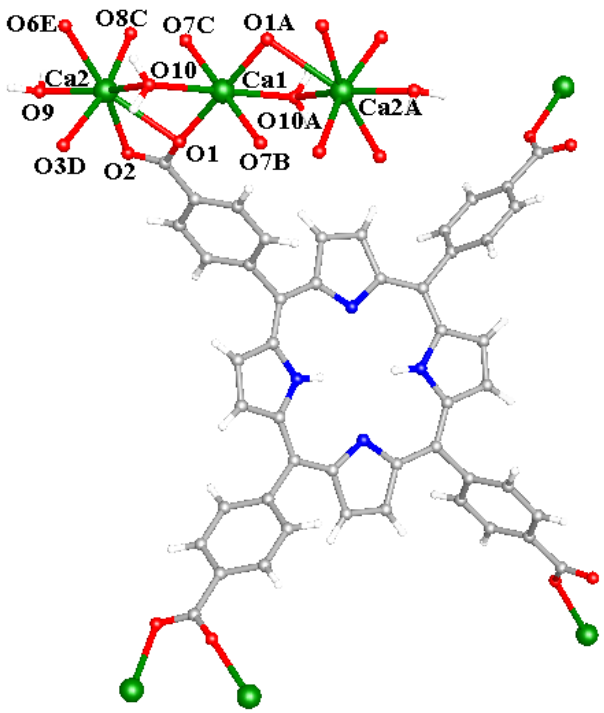


**Fig. S2** View of local coordination environment of Ca(II) ion in **1**. Symmetry codes: A = 1-X,2-Y,-Z; B = 1-X,2-Y,1-Z; C = +X,+Y,-1+Z; D = -1+X,1+Y,+Z; E = -1+X,1+Y,-1+Z.

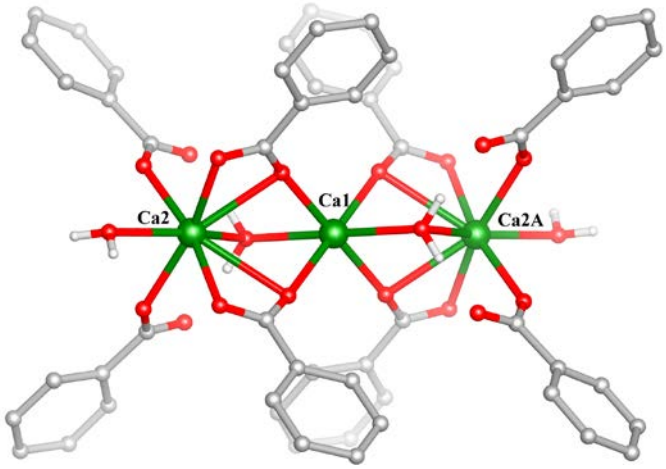


**Fig. S3** View of the {$Ca_3$} cluster in **1**. Symmetry codes: A = 1-X, 2-Y, -Z. In {$Ca_3$} cluster, Ca2 is present in form of two symmetrical equivalents, and Ca1 is located at the central position (a special position with 0.5-occupancy). Ca1 coordinates to four carboxylate oxygen atoms from four $H_2$TCPP ligands and two water molecules, resulting in a six-coordinated geometry. Ca2 is linked by six carboxylate oxygen atoms from four $H_2$TCPP ligands and two coordinated water molecule to complete an eight-coordinated geometry.

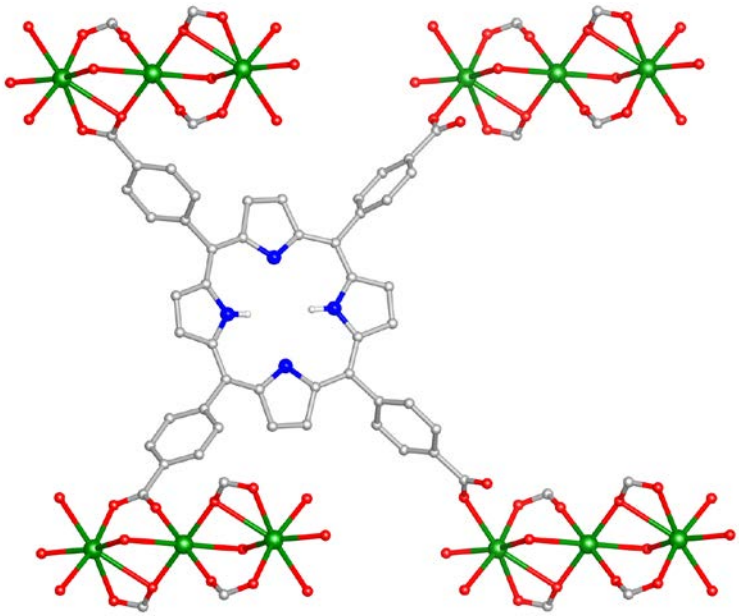

**Fig. S4** The $H_2TCPP$ ligand adopts a $\mu_7$-bridging mode to bind to four {$Ca_3$} clusters through one $\mu_2$-$\eta^1$:$\eta^1$, one $\mu_2$-$\eta^1$:$\eta^2$ and two $\mu_1$-$\eta^1$:$\eta^0$ coordination modes for its four carboxylate groups, respectively.

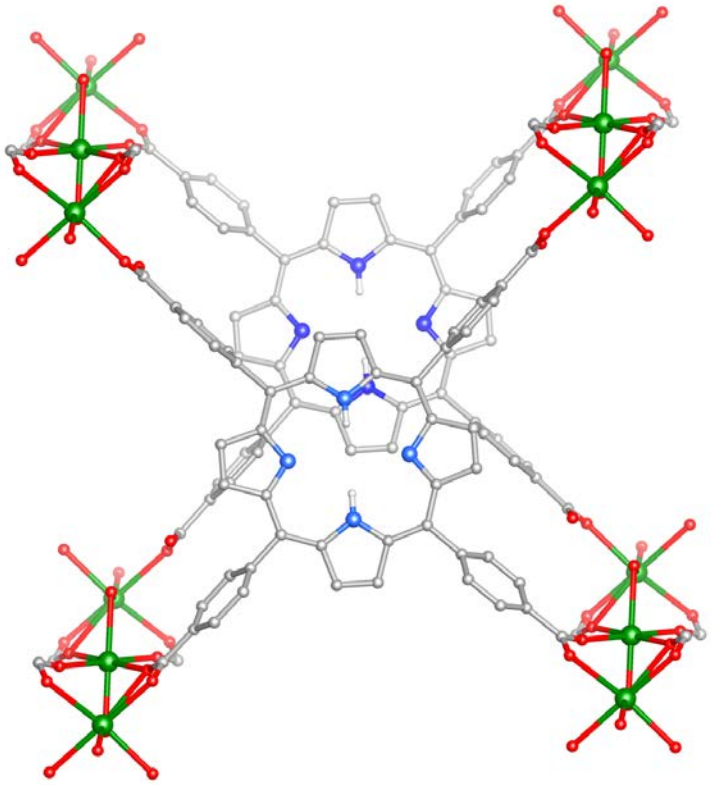

**Fig. S5** Pairs of $H_2TCPP$ ligands are tightly fixed by four rigid {Ca3} clusters.

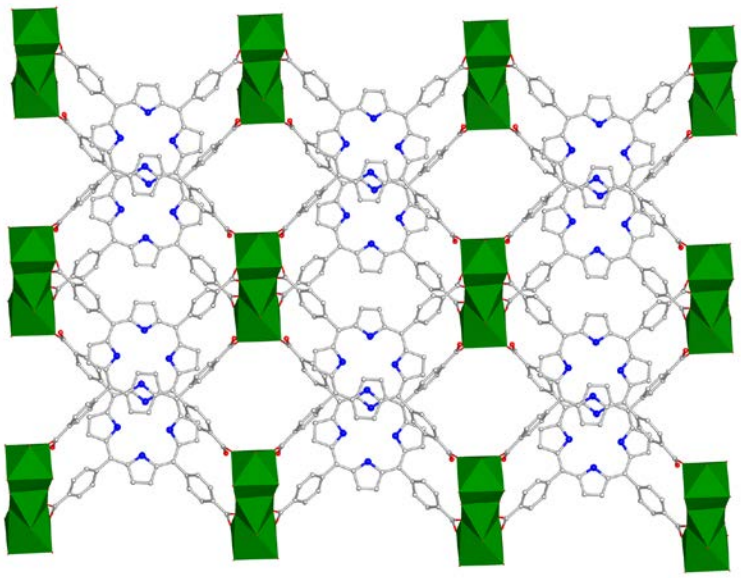

**Fig. S6** View of single layer of 1 along *a* direction.

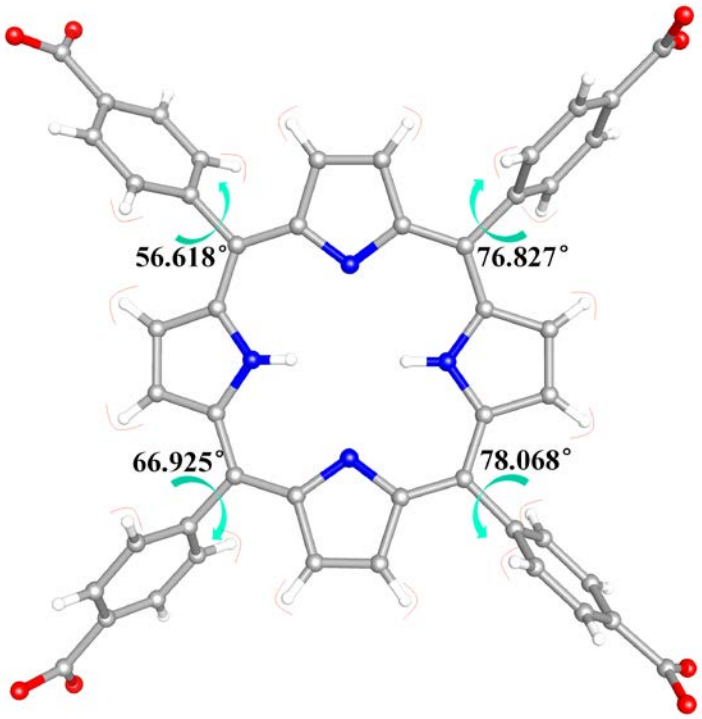


**Fig. S7** The four benzoate groups are oblique crossing to the porphyrin core with dihedral angles of 56.62, 66.92, 76.83 and 78.07°in **1**, respectively.

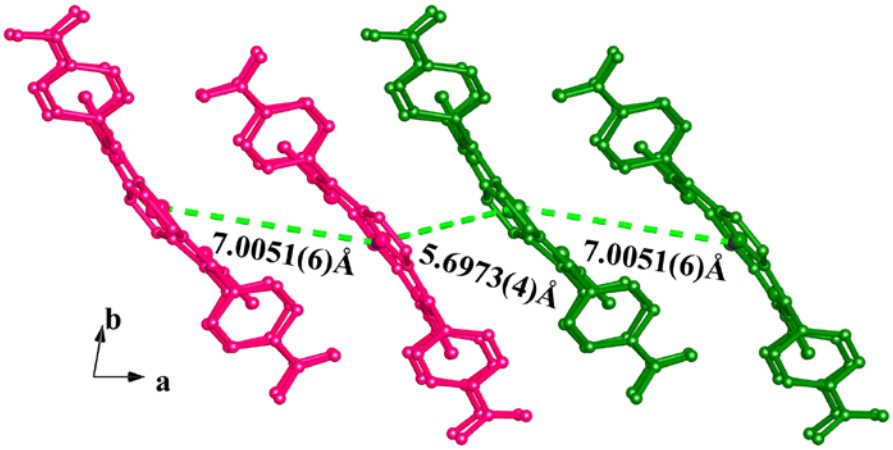


**Fig. S8** In **1**, there are two kinds of mutually parallel $H_2TCPP$ ligands that are closely positioned in space, originating from the same and two neighbouring 2D layers, respectively. The interplanar distance is about 5.6973 and 7.0051 Å, respectively.

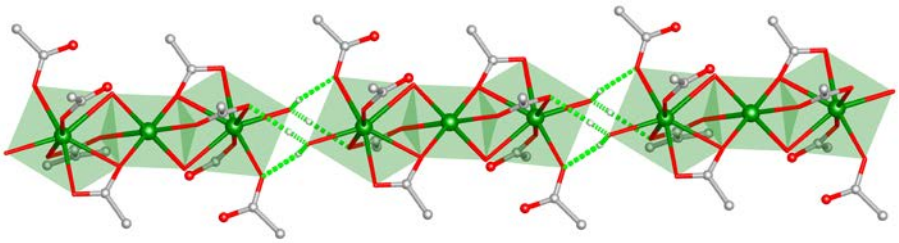

**Fig. S9** A supramolecular chain formed by the extension of {Ca3} clusters along *a* direction by means of the hydrogen bonds.

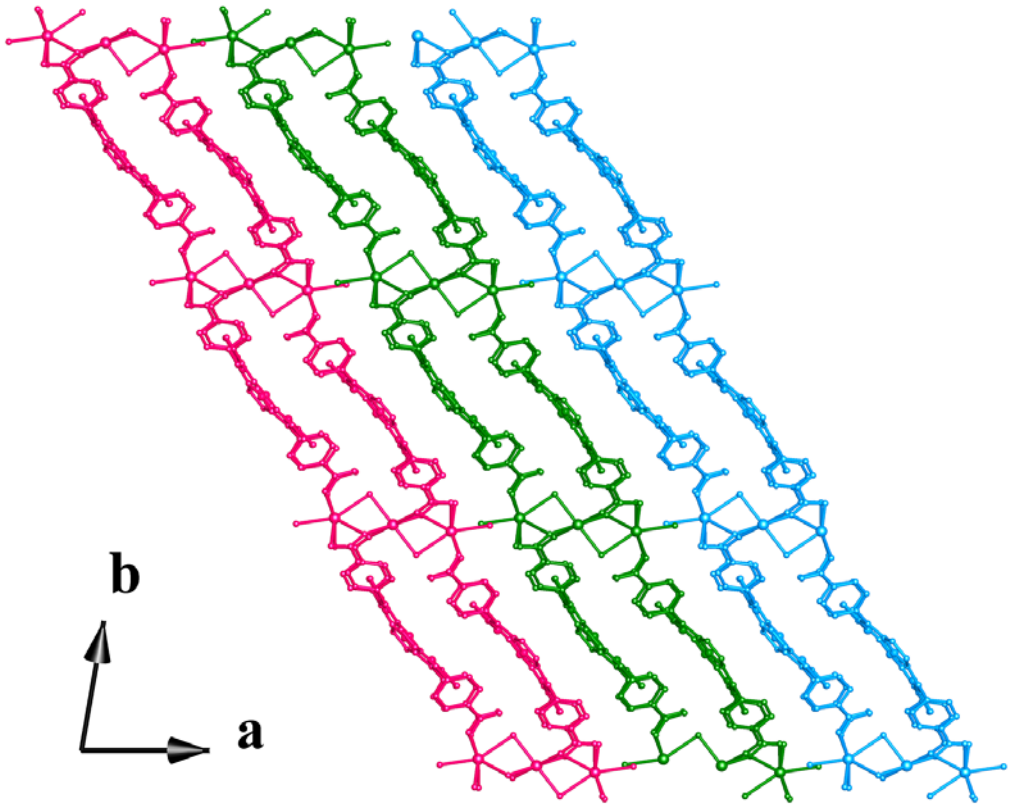


**Fig. S10** The projection of structure arrangement in **1** along the (001) direction.

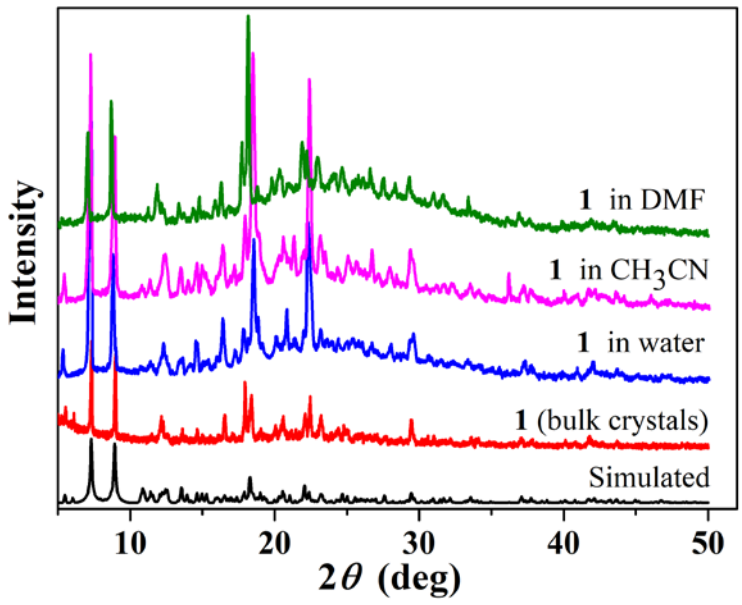


**Fig. S11** PXRD patterns of **1** after soaking in water and organic solvents for three days.

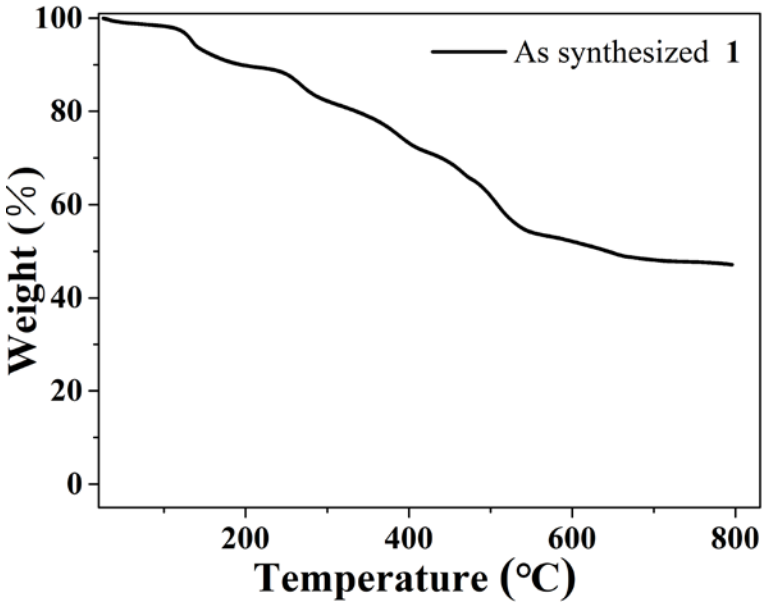


**Fig. S12** Thermogravimetric (TG) analyses curves of **1**. The first loss 6.0% occurs before 140 ºC, which is attributed to the loss of coordinated waters and other solvent molecules; the second loss between 140 ºC and 350 ºC is assigned to the decompose of the ionic liquid $[BMI]^+$ cations, and the third weight loss represents the decompose of the $H_2TCPP$ ligand, leading to the framework collapse.

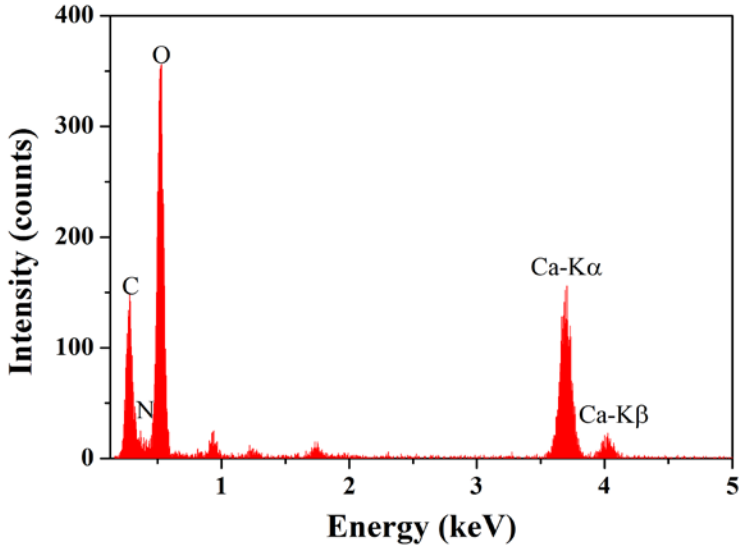


**Fig. S13** EDS analysis of **1 NSs**.

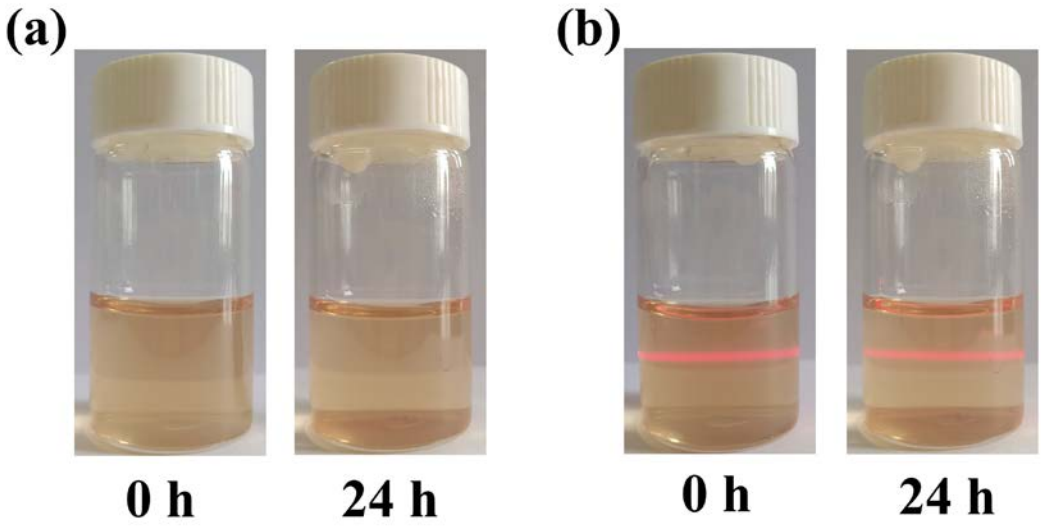


**Fig. S14** Stability evaluation of **1 NSs**. (a) Photograph of **1 NSs** that was dispersed in water for different time. (b) Tyndall effect of **1 NSs**.

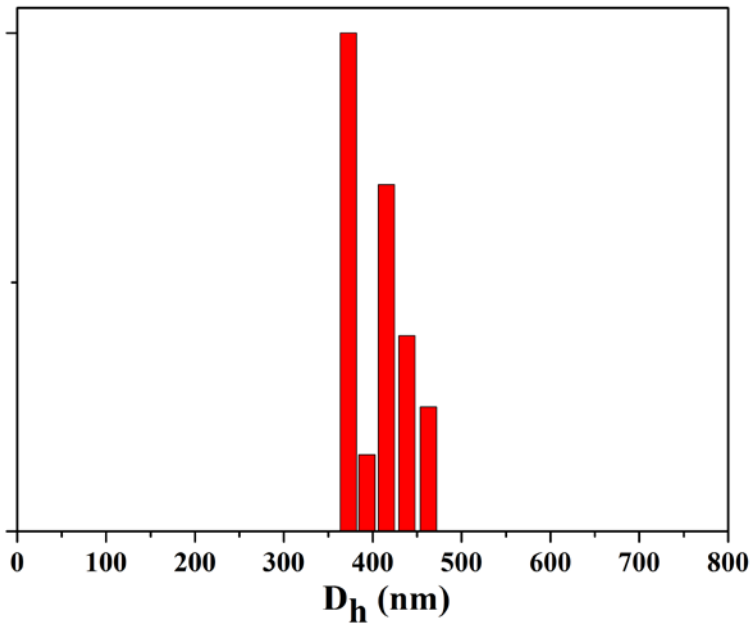


**Fig. S15** Dynamic light scattering measurement of **1 NSs** in water.

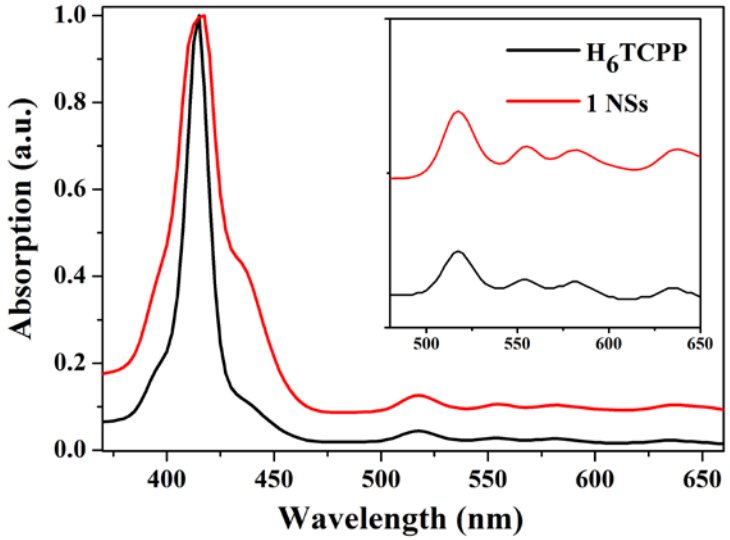


**Fig. S16** UV−visible absorption spectra of $H_6$TCPP and **1 NSs** in water solution (both at 1/3 mg/mL). Inset shows expanded views of the Q-band regions. The presence of four Q-bands and their red shifts support the presence of free-base porphyrin ligands in **1 NSs**.

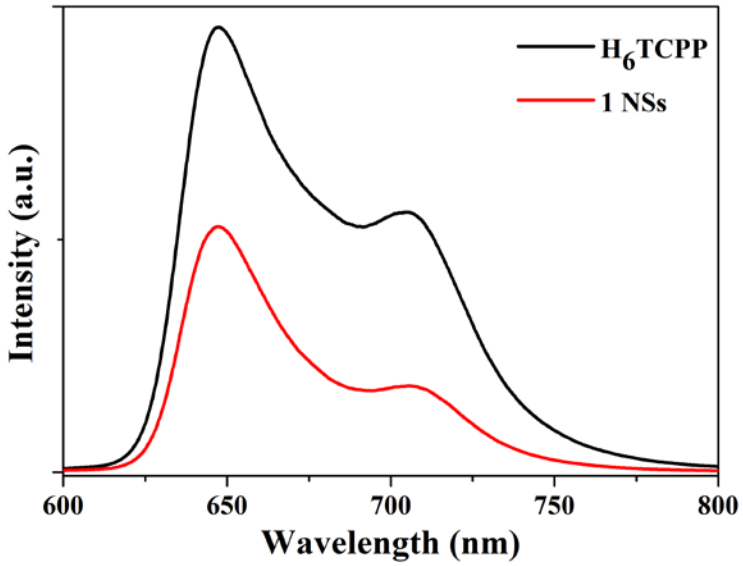


**Fig. S17** Fluorescence spectra of $H_6$TCPP and **1 NSs** in water solution (both at 1/3 mg/mL) when excited at 520 nm.

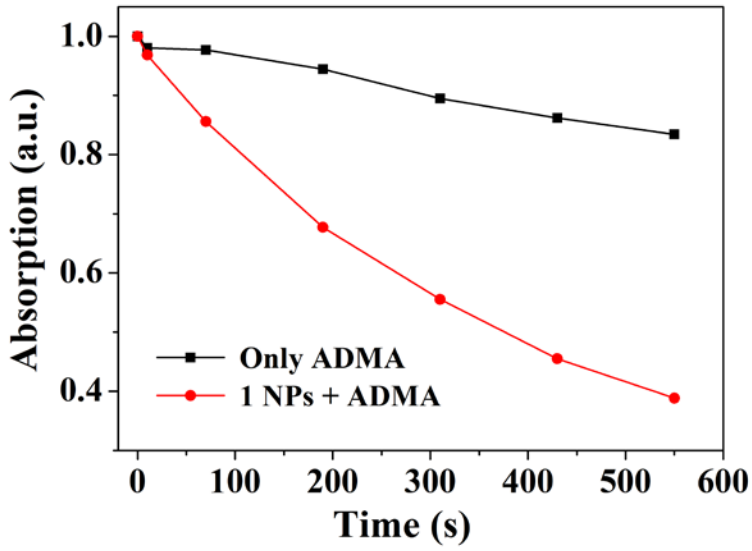


**Fig. S18** Time-dependent absorption intensities of ADMA upon irradiation in the presence of **1 NSs**.

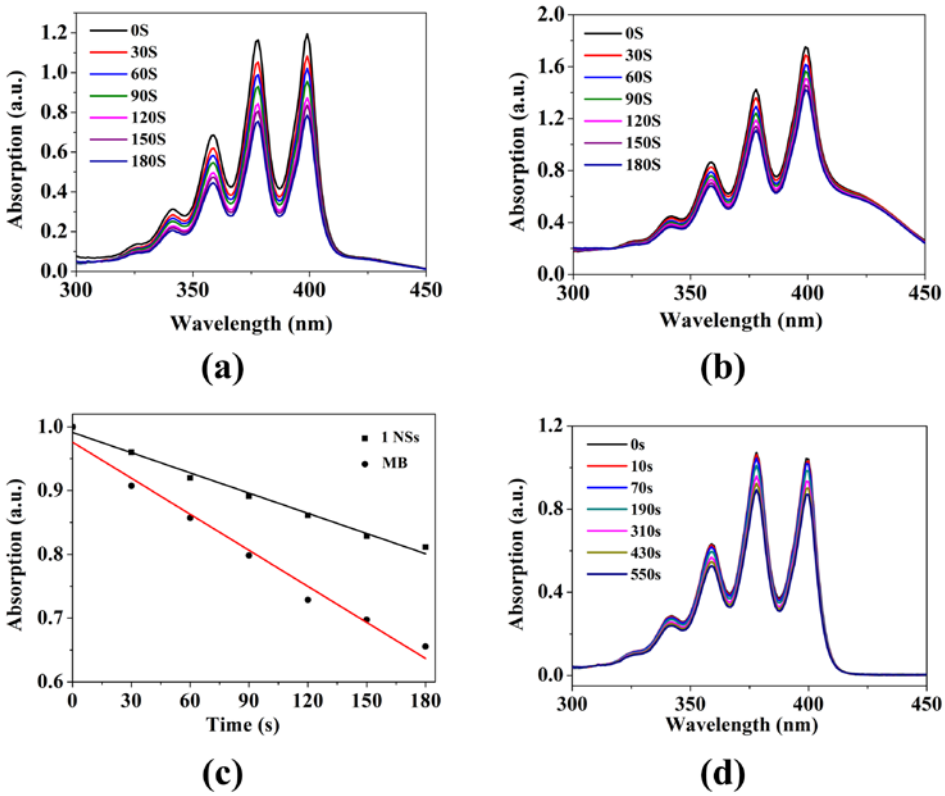


**Fig. S19** The singlet oxygen production efficiency of **1 NSs** in aqueous solution. Absorbance of ADMA after photodecomposition by ROS generation upon white light irradiation with MB (a) and **1 NSs** (b) (white light irradiation, 0.5 W $cm^{-2}$). (c) Time-dependent absorption intensity of ADMA under white light irradiation. (d) Time-dependent absorbance spectra of ADMA upon irradiation without **1 NSs**.

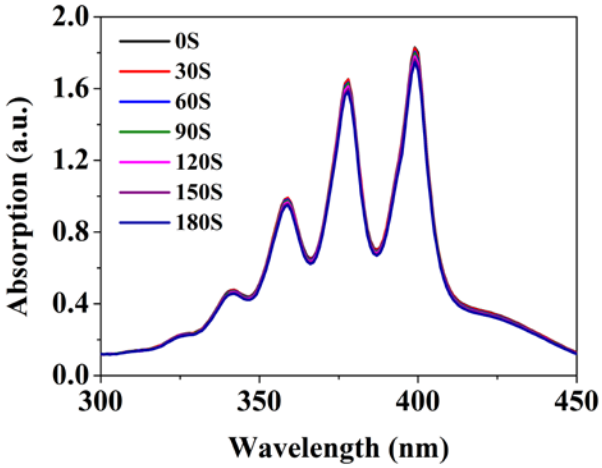


**Fig. S20** The singlet oxygen production of **1 NSs** in aqueous solution under saturated $N_2$ atmosphere upon white light irradiation (0.5 W $cm^{-2}$).

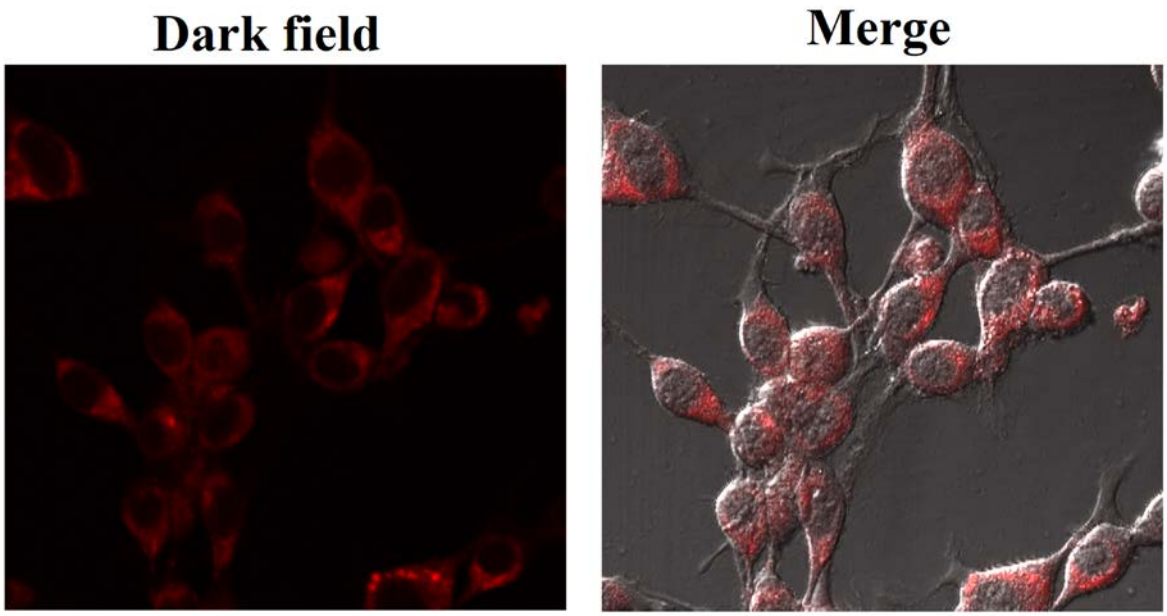


**Fig. S21** The fluorescence images of MCF-7 cells after incubated with **1 NSs**.

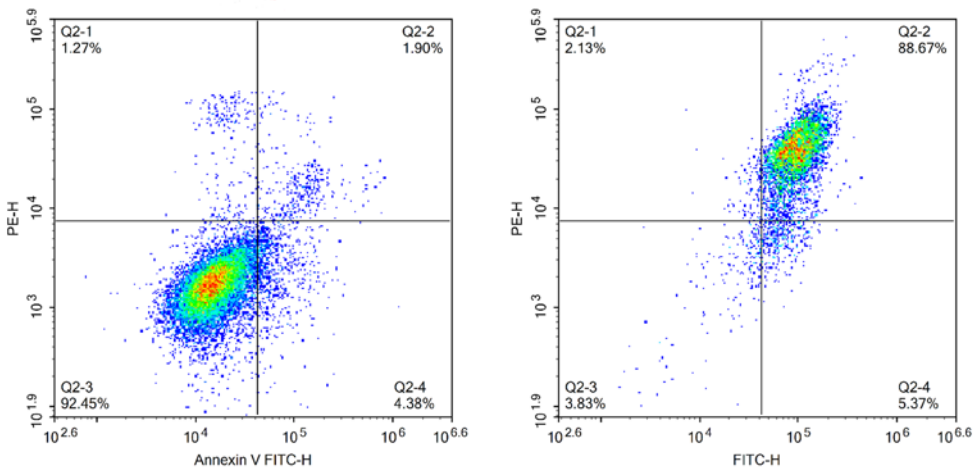


**Fig. S22** Flow cytometry analysis of MCF-7 cells incubated with **1 NSs**.

## C. Supporting Tables

**Table S1.** Crystallographic data and experimental details for **1**.

| Complex | **1** |
|---|---|
| Empirical formula | $C_{112}H_{90}Ca_3N_{12}O_{20}$ |
| Formula weight | 2044.21 |
| Temperature/K | 293(2) |
| Crystal system | triclinic |
| Space group | P-1 |
| a/Å | 11.9690(9) |
| b/Å | 15.4198(10) |
| c/Å | 17.4200(14) |
| α/° | 74.789(6) |
| β/° | 70.647(7) |
| γ/° | 76.008(6) |
| Volume/Å$^3$ | 2884.5(4) |
| Z | 1 |
| $\rho_{calc}$g/cm$^3$ | 1.017 |
| μ/mm$^{-1}$ | 0.202 |
| F(000) | 912.0 |
| Crystal size/mm$^3$ | 0.34 × 0.23 × 0.17 |
| Radiation | MoKα (λ = 0.71073) |
| 2Θ range for data collection/° | 6.548 to 56.728 |
| Index ranges | -15 ≤ h ≤ 15, -19 ≤ k ≤ 19, -22 ≤ l ≤ 22 |
| Reflections collected | 35615 |
| Independent reflections | 12349 [$R_{int}$ = 0.0771, $R_{sigma}$ = 0.1302] |
| Data/restraints/parameters | 12349/4/582 |
| Goodness-of-fit on F$^2$ | 1.031 |
| Final R indexes [I>=2σ (I)] | $R_1$ = 0.0893, $wR_2$ = 0.2197 |
| Final R indexes [all data] | $R_1$ = 0.1423, $wR_2$ = 0.2478 |

[a] $R = [\sum ||F_0| - |F_c|| / \sum |F_0|]$, $R_W = \sum w [|F_0^2 - Fc^2|^2 / \sum w (|F_w|^2)^2]^{1/2}$

**Table S2.** Selected bond distances (Å) for **1**.

| | | | |
|---|---|---|---|
| Ca1-O1[1] | 2.273(3) | Ca2-O2 | 2.460(3) |
| Ca1-O1 | 2.273(3) | Ca2-O3[4] | 2.339(3) |
| Ca1-O7[2] | 2.284(3) | Ca2-O6[5] | 2.400(3) |
| Ca1-O7[3] | 2.284(3) | Ca2-O7[2] | 2.756(3) |
| Ca1-O10[1] | 2.345(3) | Ca2-O8[2] | 2.475(3) |
| Ca1-O10 | 2.345(3) | Ca2-O9 | 2.381(3) |
| Ca2-O1 | 2.586(3) | Ca2-O10 | 2.581(3) |

Symmetry operations: [1]1-X,2-Y,-Z; [2]+X,+Y,-1+Z; [3]1-X,2-Y,1-Z; [4]-1+X,1+Y,+Z; [5]-1+X,1+Y,-1+Z.

**Table S3**. Selected bond angles (°) for **1**.

| | | | |
|---|---|---|---|
| O1-Ca1-O1[1] | 180.0 | O3[4]-Ca2-O6[5] | 92.83(12) |
| O1-Ca1-O7[2] | 99.32(12) | O3[4]-Ca2-O7[3] | 144.81(11) |
| O1-Ca1-O7[3] | 80.68(12) | O3[4]-Ca2-O8[3] | 165.73(11) |
| O1[1]-Ca1-O7[3] | 99.32(12) | O3[4]-Ca2-O9 | 83.86(11) |
| O1[1]-Ca1-O7[2] | 80.68(12) | O3[4]-Ca2-O10 | 79.44(11) |
| O1[1]-Ca1-O10[1] | 77.80(11) | O6[5]-Ca2-O1 | 145.96(11) |
| O1[1]-Ca1-O10 | 102.20(11) | O6[5]-Ca2-O2 | 162.64(11) |
| O1-Ca1-O10[1] | 102.21(11) | O6[5]-Ca2-O7[3] | 90.66(11) |
| O1-Ca1-O10 | 77.80(11) | O6[5]-Ca2-O8[3] | 83.21(10) |
| O7[2]-Ca1-O7[3] | 180.0 | O6[5]-Ca2-O10 | 79.59(10) |
| O7[3]-Ca1-O10[1] | 101.11(11) | O8[3]-Ca2-O1 | 98.83(10) |
| O7[3]-Ca1-O10 | 78.89(11) | O8[3]-Ca2-O7[3] | 49.25(9) |
| O7[2]-Ca1-O10[1] | 78.89(11) | O8[3]-Ca2-O10 | 113.09(10) |
| O7[2]-Ca1-O10 | 101.11(11) | O9-Ca2-O1 | 132.42(10) |
| O10-Ca1-O10[1] | 180.0 | O9-Ca2-O2 | 81.37(10) |
| O1-Ca2-O7[3] | 66.94(10) | O9-Ca2-O6[5] | 81.61(10) |
| O2-Ca2-O1 | 51.10(10) | O9-Ca2-O7[3] | 131.25(10) |
| O2-Ca2-O7[3] | 98.01(11) | O9-Ca2-O8[3] | 82.00(10) |
| O2-Ca2-O8[3] | 91.07(11) | O9-Ca2-O10 | 154.08(10) |
| O2-Ca2-O10 | 117.65(10) | O10-Ca2-O1 | 68.29(10) |
| O3[4]-Ca2-O1 | 92.12(12) | O10-Ca2-O7[3] | 66.80(10) |
| O3[4]-Ca2-O2 | 88.71(13) | | |

Symmetry operations: [1]1-X,2-Y,-Z; [2]1-X,2-Y,1-Z; [3]+X,+Y,-1+Z; [4]-1+X,1+Y,+Z; [5]-1+X,1+Y,-1+Z

## D. Supporting References


1 O. V. Dolomanov, L. J. Bourhis, R. J. Gildea, J. A. K. Howard and H. Puschmann, *J. Appl. Crystallogr.*, 2009, **42**, 339-341.

2 G. Sheldrick, *Acta Cryst.*, 2015, **A71**, 3-8.

3 G. Sheldrick, *Acta Cryst.*, 2015, **C71**, 3-8.